ARTICLE IN PRESS

ELSEVIER

Journal of the Mechanics and Physics of Solids
▮▮▮ (▮▮▮▮) ▮▮▮–▮▮▮

JOURNAL OF THE MECHANICS AND PHYSICS OF SOLIDS

www.elsevier.com/locate/jmps

Constitutive model for stretch-induced softening of the stress–stretch behavior of elastomeric materials

H.J. Qi, M.C. Boyce*

Department of Mechanical Engineering, Massachusetts Institute of Technology, Cambridge, MA 02139, USA

Received 1 December 2003; accepted 14 April 2004

Abstract

Elastomeric materials experience stretch-induced softening as evidenced by a pre-stretched material exhibiting a significantly more compliant response than that of the virgin material. In this paper, we propose a fully three-dimensional constitutive model for the observed softening of the stress–strain behavior. The model adopts the Mullins and Tobin concept of an evolution in the underlying hard and soft domain microstructure whereby the effective volume fraction of the soft domain increases with stretch. The concept of amplified strain is then utilized in a mapping of the macroscopic deformation to the deformation experienced by the soft domain. The strain energy density function of the material is then determined from the strain energy of the soft domain and thus evolves as the volume fraction of soft domain evolves with deformation. Comparisons of model results for cyclic simple extension with the experimental data of Mullins and Tobin show the efficacy of the model and suggest that an evolution in the underlying soft/hard domain microstructure of the elastomer captures the fundamental features of stretch-induced softening. Model simulations of the cyclic stress–strain behavior and corresponding evolution in structure with strain for uniaxial tension, biaxial tension and plane strain tension are also presented and demonstrate three-dimensional features of the constitutive model.

Keywords: Softening; Mullins' effect; Stress–strain behavior; Elastomer; Rubber

* Corresponding author. Tel: +1-617-253-2342; fax: +1-617-258-8742.
E-mail address: mcboyce@mit.edu (M.C. Boyce).

0022-5096/$ - see front matter © 2004 Elsevier Ltd. All rights reserved.
doi:10.1016/j.jmps.2004.04.008

1. Introduction

The equilibrium stress–strain behavior of elastomeric materials is observed to undergo a softening with strain history. This phenomenon is referred to as stress-softening, stretch-induced softening, and/or cyclic softening. It is observed in conventional rubbery materials (Mullins and Tobin, 1957, 1965; Harwood et al., 1965; Harwood and Payne, 1966a,b; Mullins, 1969; Bueche, 1961) as well as in thermoplastic elastomers such as thermoplastic polyurethanes (Yokoyama, 1978; Bonart and Muller-Riederer, 1981; Qi and Boyce, 2004) and thermoplastic vulcanizates (Boyce et al., 2001a,b). In rubbery materials, the softening of the equilibrium stress–strain curve is referred to as the "Mullins' effect", so named due to the comprehensive study of this behavior by Mullins on unfilled and filled rubbers during the 1950s and the 1960s (Mullins and Tobin, 1957, 1965; Harwood et al., 1965; Harwood and Payne, 1966a,b; Mullins, 1969). Fig. 1 illustrates the characteristic features of the softening of the equilibrium nominal stress-nominal strain behavior of elastomeric materials as observed in a uniaxial tension test. Three stress–strain curves, each on the same material to a final nominal strain of 3.0 are depicted: Curve 1 gives the monotonic stress–strain behavior of the material having had no prior strain history; Curve 2 gives the reloading stress–strain behavior of the material after having been initially subjected to a prior strain of 1.2; Curve 3 gives the reloading stress–strain behavior after having been subjected to a prior strain of 2.0. The reloading curves exhibit several key features:

- After having been subjected to a prior strain, the material exhibits a more compliant response at strains smaller than the maximum strain incurred in its prior strain history.
- During reloading, as the reloading strain approaches the maximum strain seen in its prior strain history, the stress–strain behavior begins to stiffen and rejoin the reference virgin curve; upon reaching the reference virgin curve, the stress–strain behavior follows that of the virgin stress–strain behavior.
- A larger prior strain gives a larger increase in compliance (greater softening of the response) upon reloading.

Although Mullins identified softening to occur in both unfilled and filled elastomers, its effect is far more pronounced in filled elastomers and therefore is frequently identified to be a filled elastomer phenomenon.

At present, most softening theories are based on two concepts. The first theory originates from Blanchard and Parkinson (1952) and Bueche (1960, 1961), who considered the increase in stiffness produced by stiff filler particles to be a result of rubber-filler attachments providing additional restrictions on the crosslinked rubber network. They attributed softening to result from the breakdown or loosening of some of these attachments. Bueche (1960, 1961), Dannenberg (1974), and Rigbi (1980) generalized the softening to be a result of strain-induced relative motion of carbon and rubber, and in some cases local separation of carbon black particles and rubber. Simo (1987), Govindjee and Simo (1991, 1992), and Miehe and Keck (2000), and Lion (1996, 1997) extended the Bueche concept and developed damage-based constitutive

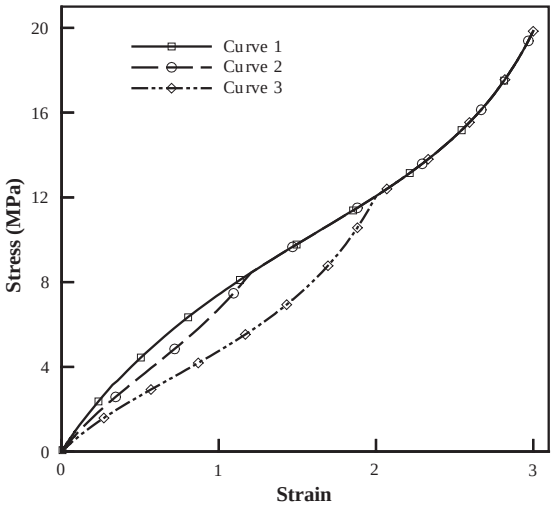

Fig. 1. Schematic of the Mullins effect observed in cyclic uniaxial tension tests: Curve 1 shows the monotonic stress–strain behavior; curve 2 shows unloading from a strain of 1.2 followed by loading to a strain of 3.0; curve 3 shows unloading from a strain of 2.0 followed by loading to a strain of 3.0. Symbols are included on the curves in order to help distinguish overlapping curves.

models to simulate the material behavior within the framework of large strain continuum mechanics.

The second theory posed to explain the softening phenomenon is due to Mullins and coworkers (Mullins and Tobin, 1957, 1965; Harwood et al., 1965; Harwood and Payne, 1966a,b; Mullins, 1969). They consider softening to be an evolution in soft and hard domains within the elastomer whereby stretch produces a quasi-irreversible rearrangement of molecular networks due to localized nonaffine deformation resulting from short chains reaching the limit of their extensibility. This nonaffine deformation produces a displacement of the network junctions from their initial state, which thus produces some form of rearrangement of hard and soft domains in the elastomeric phase with strain, acting to increase the effective volume fraction of soft domain. The concept of a phase transition with strain has been used by Wineman and coworkers (Rajagopal and Wineman, 1992; Wineman and Huntley, 1994) to capture the destruction and rebuilding of the underlying molecular network upon reaching critical strain values. The concept of hard/soft domain reorganization with strain has been used as motivation in the models of Beatty and coworkers (Johnson and Beatty, 1993a,b; Beatty and Krishnaswamy, 2000) who consider molecular chains to be pulled out from clusters and transformed into soft regions, and of Marckmann et al. (2002) who propose a network alteration whereby molecular chain density decreases and the average number of monomer segments in a molecular chain increases, and of Ogden and coworkers (Ogden and Roxburgh, 1999a,b; Dorfmann and Ogden, 2003; Horgan et al., 2004) who combine the concept of hard/soft domain reorganization with the damage approach.

In the Mullins approach, filled rubbers were treated as a composite system and the concept of amplified strain was used to explain the enhanced softening phenomenon observed in filled rubbers. In filled elastomers, the average strain (or alternatively, stretch) in the elastomeric domains is necessarily amplified over that of the macroscopic strain since the stiff filler particles accommodate little of the macroscopic strain. For uniaxial tension loading, the amplified elastomer stretch is taken to be $\Lambda = 1 + X(\lambda - 1)$, where X is an amplification factor dependent on particle volume fraction and distribution and λ is the macroscopic axial stretch. These researchers (Harwood et al., 1965) proposed that cyclic softening was a property of the unfilled vulcanizate and was magnified through the amplified strain for filled rubbers, thus producing an apparently greater degree of softening at any given macroscopic strain when compared to the corresponding unfilled elastomer.

Based on the concept of amplified strain, Mullins and Tobin (1957) in their very early work suggested that the softening in rubber vulcanizates was due to the decrease of volume fraction of effective hard domain, v_f, as a result of conversion of hard domain to soft domain. Recently, micro-mechanics studies on filled elastomers and filled polymers conducted by Boyce and coworkers (Bergstrom and Boyce, 1999, 2000; Boyce et al., 2001a,b) have provided some additional insights into possible hard/soft transition mechanisms. Micromechanical modeling of rigid particle filled elastomers by Bergstrom and Boyce (1999) reveals the entrapment of rubber domains within aggregates of stiff particles, thus resulting in the effective volume fraction of stiff particles to be larger than the physical fraction, i.e., the "occluded volume" effect postulated by earlier workers (Medalia and Kraus, 1994). Evolution in particle distribution with deformation could release occluded volumes of rubber and thus soften the material. Regions of stiffer vs. more compliant elastomer domains in unfilled elastomers could be thought to evolve in a similar manner. In a study of cyclic softening in thermoplastic vulcanizates (TPVs), where the vulcanizates are the filler particles, Boyce et al. (2001a,b) showed that the softening is due to the gradual evolution in particle/matrix configuration due to straining during previous loading cycles. The plastic deformation of the contiguous thermoplastic phase acted to "release" vulcanizate particles creating a pseudo-continuous vulcanizate phase and thus a softer response during subsequent cycles. Although the material in the TPV study is a system of soft fillers/hard matrix, these micromechanical simulations demonstrate how an evolution in soft/hard microstructures can result in softening of the macroscopic mechanical response.

In this paper, we pursue Mullins' early concept and propose a constitutive model where the softening of the equilibrium stress–stretch behavior is due to an evolution of the effective volume fraction of the soft domain during the deformation process whereupon occluded soft material domains are released during deformation due to the relative motions and deformation of the hard domains. Model predictions of the evolution in structure and corresponding stress–stretch behaviors under cyclic uniaxial loading are shown first; comparisons between model and experimental data from the literature are then presented. The three-dimensional nature of the model is illustrated in simulations of uniaxial tension, equibiaxial tension and plane strain tension.

2. Constitutive model description

Constitutive relationships between stress and strain for the equilibrium behavior of elastomeric materials are most often expressed in terms of strain energy density, U, where U is expressed as a function of deformation and material properties. Here, we follow that approach and further develop stretch invariant based strain energy density functions to include the effects of stretch-induced softening using the Mullins–Tobin concept of hard/soft domains.

The deformation of a material point may be described by the deformation gradient $\mathbf{F} = \mathrm{d}\mathbf{x}/\mathrm{d}\mathbf{X}$, where $\mathbf{x}$ represents the current position and $\mathbf{X}$ represents the reference position. The left Cauchy Green strain tensor is given by $\mathbf{B}=\mathbf{F}\mathbf{F}^{\mathrm{T}}$. The stretch invariants are given by

$$I_1 = \mathrm{tr}\,\mathbf{B} = \lambda_1^2 + \lambda_2^2 + \lambda_3^2, \tag{1a}$$

$$I_2 = \mathrm{tr}\,\mathbf{B}^{-1}\,\det\mathbf{B} = \lambda_1^2\lambda_2^2 + \lambda_2^2\lambda_3^2 + \lambda_1^2\lambda_3^2, \tag{1b}$$

$$I_3 = \det\mathbf{B} = \lambda_1^2\lambda_2^2\lambda_3^2, \tag{1c}$$

where λ_i are the principal stretches. Here, we will limit our study to the case of incompressible materials; thus, $I_3 = 1$. Therefore, the strain energy density for an isotropic incompressible elastomer can be expressed as a function of I_1 and I_2: $U = \hat{U}(I_1, I_2)$. In elastomeric materials, the first invariant I_1 has been found to be a far stronger contributor to strain energy density than the second invariant and therefore we will focus on I_1-based strain energy density functions in this study

$$U = U(I_1). \tag{2}$$

In particular, as a starting point, we will consider the Arruda–Boyce eight chain model:

$$U = \mu\left[\sqrt{N}\lambda_{\mathrm{chain}}\beta + N\ln\frac{\beta}{\sinh\beta}\right], \tag{3}$$

$$\mu = nk\Theta, \quad \beta = \mathsf{L}^{-1}\left(\frac{\lambda_{\mathrm{chain}}}{\sqrt{N}}\right),$$

where L is the Langevin function defined as $\mathsf{L}(\beta) = \coth\beta - 1/\beta$. This model is based on the statistics of the underlying macromolecular network where n is chain density (number of molecular chains per unit reference volume), N is the number of "rigid links" between two crosslinks (and/or strong physical entanglements), $\lambda_{\mathrm{chain}} = \sqrt{I_1/3}$ is the stretch on each chain in the eight chain network, k is Boltzmann's constant, and Θ is absolute temperature. The Cauchy stress, $\mathbf{T}$, is obtained by proper differentiation of the strain energy density

$$\mathbf{T} = 2\frac{\mathrm{d}U}{\mathrm{d}I_1}\mathbf{B} - p\mathbf{I}, \tag{4}$$

where p is the additional pressure determined by satisfying the boundary conditions. For the case of uniaxial tension the Arruda–Boyce model gives the axial Cauchy (true)

stress–stretch relationship:

$$\sigma = \frac{\mu}{3}\frac{\sqrt{N}}{\lambda_{\text{chain}}}\mathsf{L}^{-1}\left(\frac{\lambda_{\text{chain}}}{\sqrt{N}}\right)\left(\lambda^2 - \frac{1}{\lambda}\right),$$

where

$$\lambda_{\text{chain}} = \sqrt{\frac{1}{3}\left(\lambda^2 + \frac{2}{\lambda}\right)}, \tag{5}$$

where σ is the true axial stress and λ is the macroscopic axial stretch.

As indicated earlier, Mullins and Tobin (1957) introduced the notion of amplified strain (or stretch) to capture the effects of rigid filler particles on the uniaxial stress–stretch behavior of elastomers. The amplified axial stretch was given by

$$\Lambda = 1 + X(\lambda - 1), \tag{6}$$

where Λ is the amplified stretch (the average stretch in the matrix), and X is the amplification factor which depends on filler volume fraction and distribution. Following their procedure, the stress–stretch behavior of a rigid particle filled elastomer is then obtained by replacing λ with Λ in the axial stress–stretch constitutive model. The Mullins and Tobin concept of amplified strain was based on earlier work of several investigators on small strain modulus enhancement due to the presence of rigid fillers. Following the earlier work of Einstein (1906, 1911) on viscosity of particle-filled viscous fluids, Smallwood (1944) estimated the effective small strain Young's modulus $\langle E\rangle$ of a rigid particle filled solid to be

$$\langle E\rangle = E_{\text{m}}(1 + 2.5v_{\text{f}}), \tag{6′}$$

where E_{m} is the Young's modulus of the matrix material and v_{f} is the volume fraction of the rigid filler. A number of attempts of various levels of sophistication have been conducted to incorporate interactions between neighboring particles to predict the effective modulus of a composite with a high volume fraction of rigid filler. One of the most cited models for spherical rigid fillers is the Guth–Gold model (Guth and Simha, 1936; Guth and Gold, 1938; Guth, 1945),

$$\langle E\rangle = E_{\text{m}}(1 + 2.5v_{\text{f}} + 14.1v_{\text{f}}^2). \tag{7}$$

The Mullins and Tobin model of the large stretch behavior of the filled elastomers capitalizes upon the modulus enhancement models by taking the strain amplification factor to be that of the modulus enhancement factor: for example, taking $X = 1 + 2.5v_{\text{f}} + 14.1v_{\text{f}}^2$. More recent models (for example, Budiansky, 1965; Mori and Tanaka, 1973; Suquet, 1997; Ponte Castaneda, 1989), some of which estimate an effective strain in the soft phase, offer a higher level of analytical sophistication, and yield the same basic form as Eq. (7) (see Bergstrom and Boyce (1999) for a review and comparison of some of these models).

In the Mullins and Tobin work (1957), it is the uniaxial stretch being amplified. Bergstrom and Boyce (1999) extended this theory to a general three-dimensional deformation state, where the first invariant of the stretch is amplified by

$$\langle I_1\rangle_{\text{m}} = X(\langle I_1\rangle - 3) + 3, \tag{8}$$

where $\langle I_1\rangle_m$ is the average I_1 in the matrix, and $\langle I_1\rangle$ is the overall macroscopic I_1 of the composite material. Depending on the shape and properties of fillers, and interactions among particles, X can take a general polynomial form of $X = 1 + av_f + bv_f^2$. The amplified $\langle I_1\rangle_m$ thus can be applied to any I_1-based hyperelastic model. For a neo-Hookean matrix with rigid particles, the strain energy density of the composite $\langle U\rangle$ is found from the strain energy of the matrix $\langle U_m\rangle$ and is given as

$$U = (1 - v_f)\langle U_m\rangle = (1 - v_f)\frac{\mu_m}{2}[\langle I_1\rangle_m - 3] = (1 - v_f)X\frac{\mu_m}{2}(\langle I_1\rangle - 3). \tag{9}$$

For the case of a dilute solution, for this approach to reduce to the corresponding modulus enhancement model, the quantity $(1 - v_f)X$ should approach $(1 + 2.5v_f)$ as $v_f \to 0$, resulting in $a = 3.5$. Therefore,

$$X = 1 + 3.5v_f + bv_f^2, \tag{10}$$

where b is a coefficient depending on the nature of the dispersion of particles in the matrix. By comparing with the Guth–Gold model, we take $b = 18$ to characterize a system with well dispersed particles.

Applying this same approach to the Arruda–Boyce (1993) model gives a strain energy density of

$$U = v_s\mu\left[\sqrt{N}\Lambda_{chain}\beta + N\ln\frac{\beta}{\sinh\beta}\right], \tag{11}$$

where the amplified chain stretch is given by

$$\Lambda_{chain} = \sqrt{X(\bar{\lambda}^2 - 1) + 1} \tag{12a}$$

and

$$\beta = \mathsf{L}^{-1}(\Lambda_{chain}/\sqrt{N}), \tag{12b}$$

where $\bar{\lambda}^2 = I_1/3$ and I_1 is the first invariant of the macroscopic $\mathbf{B}$. μ is the initial modulus of the soft domain regions, N is the number of rigid links between crosslinks of the soft domain region, $X = 1 + 3.5(1 - v_s) + 18(1 - v_s)^2$, and v_f has been replaced by $1 - v_s$ and v_s is the volume fraction of the soft domains. The Cauchy stress is obtained by properly differentiating the strain energy function of Eq. (11) using Eq. (4):

$$\mathbf{T} = \frac{v_s X\mu}{3}\frac{\sqrt{N}}{\Lambda_{chain}}\mathsf{L}^{-1}\left(\frac{\Lambda_{chain}}{\sqrt{N}}\right)\mathbf{B} - p\mathbf{I}. \tag{13}$$

For the case of a uniaxial loading, the axial Cauchy stress as a function of the macroscopic axial stretch is given by

$$\sigma = \frac{v_s X\mu}{3}\frac{\sqrt{N}}{\Lambda_{chain}}\mathsf{L}^{-1}\left(\frac{\Lambda_{chain}}{\sqrt{N}}\right)(\lambda^2 - \lambda^{-1}). \tag{14}$$

In order to capture the effect of stretch-induced softening, we now invoke the concept of hard and soft domains within the elastomer and the evolution of the hard and soft domain configuration with stretch. The volume fraction of soft domains v_s is taken to evolve with deformation where initially occluded regions of soft domains are gradually released with deformation. We take the current structural state to be characterized by Λ_{chain}^{max}, the maximum local chain stretch in the deformation history. We also assume that

once an occluded soft domain is released or transformed from the hard domain, it will not relapse to the original occluded configuration upon unloading, i.e. the configuration change of hard domain to soft domain is taken to be permanent.[1] v_s thus remains at its value attained at the maximum chain stretch encountered during its loading history. Evolution in v_s will be re-activated once the material structure further evolves; structure evolution is taken to recommence once the local chain stretch exceeds the previous maximum chain stretch, i.e. when $\Lambda_{chain} \geqslant \Lambda_{chain}^{max}$. Therefore, when $\Lambda_{chain} \geqslant \Lambda_{chain}^{max}$, v_s is modeled to increase with increasing Λ_{chain}^{max}, which is updated to be $\Lambda_{chain}^{max} = \Lambda_{chain}$, and thus the amplification factor X decreases with increasing Λ_{chain}^{max}. The evolution of v_s is assumed to take a modified form of saturation type evolution rule (e.g., Miehe and Keck, 2000), which has the form

$$\dot{v}_s = A(v_{ss} - v_s)\dot{\Lambda}_{chain}^{max}, \tag{15}$$

where A is a parameter that characterizes the evolution in v_s with increasing Λ_{chain}^{max} and v_{ss} is the saturation value of v_s. Here, in order to capture the observed dependence of softening rate on stretch, Eq. (15) is modified to be[2]

$$\dot{v}_s = A(v_{ss} - v_s)\frac{\lambda_{chain}^{lock} - 1}{(\lambda_{chain}^{lock} - \Lambda_{chain}^{max})^2}\dot{\Lambda}_{chain}^{max}, \tag{16a}$$

where $\lambda_{chain}^{lock} = \sqrt{N}$ is the locking stretch of a molecule chain, and

$$\dot{\Lambda}_{chain}^{max} = \begin{cases} 0, & \Lambda_{chain} < \Lambda_{chain}^{max}, \\ \dot{\Lambda}_{chain}, & \Lambda_{chain} \geqslant \Lambda_{chain}^{max}. \end{cases} \tag{16b}$$

Note, as $\Lambda_{chain}^{max} \to \lambda_{chain}^{lock}$, $(v_{ss} - v_s) \to 0$ at a faster rate than $(\lambda_{chain}^{lock} - \Lambda_{chain}^{max})^2 \to 0$, therefore $\dot{v}_s \to 0$, as $(v_{ss} - v_s) \to 0$.

Note that the strain energy is still given by Eq. (11) and the Cauchy stress is still given by Eq. (13) where the structure v_s now evolves with deformation. This structural evolution is taken to be irreversible. Although the Cauchy stress is given by Eq. (13), the evolving nature of v_s adds additional subtlety to the thermodynamics that lead to the differentiation of the strain energy density function U needed to obtain the stress $\mathbf{T}$; the formulation is detailed in Appendix A for completeness.

It is noted that, as shown by Mullins (1948) and James and Green (1975), stretch induced softening demonstrates a certain level of anisotropy. Although the model proposed in this paper will capture a dependence of softening on the state of imposed strain (e.g., uniaxial tension, simple shear, uniaxial compression), it does not address the issue of developing material anisotropy with softening. However, the proposed model does provide insight into the mechanism of anisotropic softening. The concept of effective volume fraction of soft domain originates from the inhomogeneous distribution of strain in the microscopically heterogeneous material. The effective volume

[1] In reality, there is a very long time constant to recover back to the original state. This recovery time constant is far greater than the time period of interest here and we thus take the softening to be irreversible.

[2] Eqs. (10), (12) and (16) are solved by forming a nonlinear equation, $\Lambda_{chain} = g(\bar{\lambda}, \Lambda_{chain})$, which can be solved numerically using fixed point iteration for a given $\bar{\lambda} = \sqrt{I_1/3}$ with Λ_{chain} from the previous increment as the initial value for the iteration.

Table 1
Material parameters used in Fig. 2

μ (MPa)	N	A	v_{s0}	v_{ss}
1.00	14.0	0.7	0.4	0.85

fraction of soft domain will evolve most effectively to enable deformation of maximum principle stretching, thus creating a stretching-direction sensitive evolution of effective soft domain and producing anisotropy in the stress–strain behavior. In this paper, we simply assume the evolution of effective volume fraction of soft domain is isotropic.

3. Results

The behavior of the constitutive model is now shown in several deformation simulations. First, we take a representative (fictitious) material and demonstrate key features of the model prediction of the stress–strain behavior and the stretch-induced evolution of effective volume fraction of soft domain during cyclic deformation. Second, the model is then fit to the classic Mullins and Tobin (1957) uniaxial tension data to demonstrate its ability to capture real material behavior. Finally, the model predictions of various deformations (uniaxial tension, equibiaxial tension, and plane strain tension) are compared.

3.1. Demonstration of basic model features

To illustrate the behavior of this constitutive model, we first consider the axial loading of a representative material with the properties given in Table 1. Two cases are considered: one where the volume fraction of soft domain does not evolve with deformation and one where the volume fraction evolves with deformation according to Eq. (16). Fig. 2 shows the equilibrium stress–strain response for the two cases (Fig. 2(a)) together with the corresponding evolution in effective volume fraction of soft domain in Fig. 2(b). The stiffest stress–strain behavior (curve 1) corresponds to the simulation where v_s is taken to be constant at 0.40; in this case, the unloading and reloading behaviors are identical to the initial loading behavior. For the case where v_s is taken to increase with stretch, the stress–strain response is observed to exhibit a more compliant response than when v_s is held constant since, even during the initial loading stage, the volume fraction of soft domain is increasing with strain as shown in Fig. 2(b). Upon unloading, v_s is taken to be that obtained at the largest stretch achieved (i.e. the $v_s = 0.74$ value obtained due to the initial strain excursion of 2.0 (curve 2)) and thus the stress–strain curve is more compliant during unloading than that observed during the initial loading (where v_s had been evolving from a value of 0.4 to the value of 0.74). The stress–strain curve during reloading (curve 3) is identical to the unloading curve and is observed to rejoin the stress–strain curve of the initial excursion when reaching the maximum strain of 2.0 incurred during the initial strain excursion.

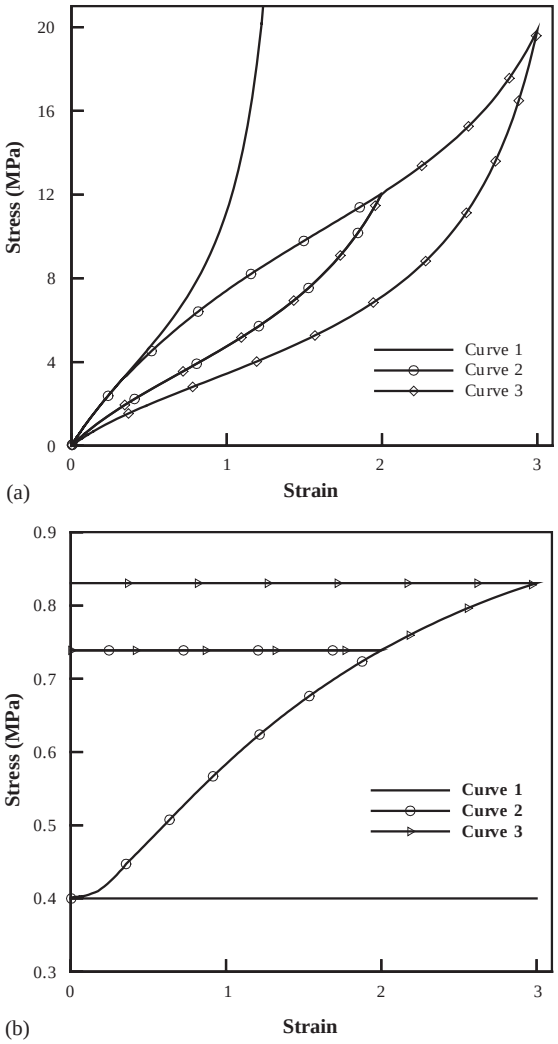

Fig. 2. Effects of evolution of effective volume fraction to the stress–strain response: (a) Stress–strain curves; (b) evolution of effective volume fraction of soft domains. In both figures, curve 1 shows the results where effective volume fraction does not evolve; curve 2 shows the results of loading to nominal strain of 2.0 then unloading; curve 3 shows reloading to nominal strain of 3.0 from previously loading to nominal strain of 2.0 and unloading.

Upon increasing the strain beyond 2.0, the stress–strain curve is observed to rollover and follow the path that an initial strain excursion to larger strain would have taken; as shown in Fig. 2(b), the v_s is observed to begin to increase with strain again when the reloading strain exceeds the maximum strain of the initial strain excursion (curve 3 in Fig. 2(b)). The stress–strain behavior observed during unloading from the cycle 2 strain maximum of 3.0 is yet again more compliant. Note that this model for the evolution

Table 2
Material parameters for the vulcanizate material of Mullins and Tobin (1957)

μ (MPa)	N	A	v_{s0}	v_{ss}
1.94	21.0	0.15	0.44	0.90

in soft domain and corresponding stretch-induced softening differs substantially from that proposed by Ogden and coworkers (1999a,b, 2003a,b), who propose the softening mechanism to evolve during unloading and to evolve back to the unused state during reloading until reaching the prior maximum stretch. The evolution used in the Ogden formulation enables rejoining the virgin state stress–strain behavior since the material state is essentially modeled to return to its virgin state during reloading. The model of Beatty and coworkers (Johnson and Beatty, 1993a,b; Beatty and Krishnaswamy, 2000) takes the volume fraction of soft material to evolve during deformation and remain constant during unloading, whereby the quantity $m \equiv \sqrt{\mathrm{tr}\,\mathbf{B}^2}$ is used to monitor deformation. Beatty and coworkers then utilize a softening function as essentially a damage-like premultiplier on the strain energy function and thus on the end stress tensor. Neither the Ogden nor the Beatty approach utilizes the volume fraction of soft domain in a mapping of macroscopic deformation to deformation in the soft domain (i.e., they do not use the strain amplification factor concept proposed by Mullins and Tobin (1957)). Govindjee and Simo (1991, 1992) utilize a mapping of macroscopic deformation to microscopic deformation in their studies on particle filled elastomers, but utilize a Bueche damage approach to capture the softening phenomenon. While each of these formerly proposed approaches has merit, the approach proposed in this paper captures the basic concept of Mullins and Tobin along with some of the more attractive features of the more recent models of others and does so in a very simple manner. Below, the behavior of the new model is further demonstrated in comparisons with the experimental data of Mullins and Tobin (1957).

3.2. Comparison to Mullins and Tobin data

Uniaxial data on a vulcanizate obtained by Mullins and Tobin (1957) are adopted here to verify the proposed model.[3] A systematic method was developed to obtain the material parameters in the proposed model and is detailed in Appendix B. The obtained material parameters are listed in Table 2.

Fig. 3 shows the comparison between model predictions and experimental results. The model predicts the loading, unloading and reloading stress–strain behavior very well for all cycles. It is noted that in the material parameter identification, the reloading curve that has the largest maximum previously attained strain and the loading curve on virgin material are used. The model predictions show excellent agreement with

[3] We note that the Mullins and Tobin data are essentially "equilibrium" data; they reported a 3-min relaxation period prior to the collection of each data point used in the construction of their stress–strain curves where little additional relaxation was seen after the allotted 3 min.

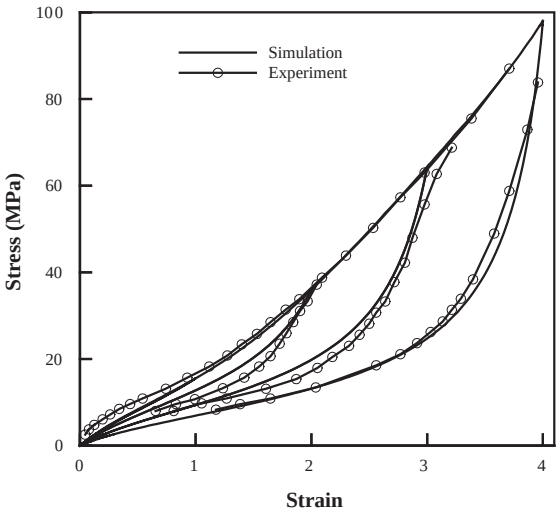

Fig. 3. Mullins and Tobin (1957) experimental results and the model predictions of cyclic nominal stress–strain behavior of a vulcanizate.

these two curves. Moreover, the model also predicts the reloading curves with smaller maximum previously attained strain very well.

3.3. Model behavior under different states of deformation

The proposed model is applicable to general multi-axial loading conditions. In order to illustrate the fully three-dimensional nature of the model, simulations of uniaxial tension, equibiaxial tension and plane strain tension were conducted.

The material is subjected to loading–unloading–reloading cycles to maximum strains of $\varepsilon=2.0$ and 3.0, and a final reloading to $\varepsilon=3.5$. For uniaxial and plane strain tension, these maximum strains correspond to the imposed axial strain; for equibiaxial tension, these maximum strains correspond to the equibiaxial tensile strains. The material parameters used are those obtained from fitting the Mullins and Tobin results.

The nominal stress (f)-stretch behavior in uniaxial tension is given by

$$f = \frac{v_s X\mu}{3}\,\frac{\sqrt{N}}{\Lambda_{\text{chain}}}\,\mathcal{L}^{-1}\!\left(\frac{\Lambda_{\text{chain}}}{\sqrt{N}}\right)(\lambda-\lambda^{-2}), \tag{17}$$

where $\Lambda_{\text{chain}}=\sqrt{\frac{X}{3}(\lambda^2+2\lambda^{-1}-3)+1}$, and λ is the axial stretch. Fig. 4(a) shows the cyclic nominal stress-nominal strain curves during uniaxial tension.

The equibiaxial nominal stress–stretch behavior is given by

$$f_1=f_2=\frac{v_s X\mu}{3}\,\frac{\sqrt{N}}{\Lambda_{\text{chain}}}\,\mathcal{L}^{-1}\!\left(\frac{\Lambda_{\text{chain}}}{\sqrt{N}}\right)(\lambda-\lambda^{-5}), \tag{18}$$

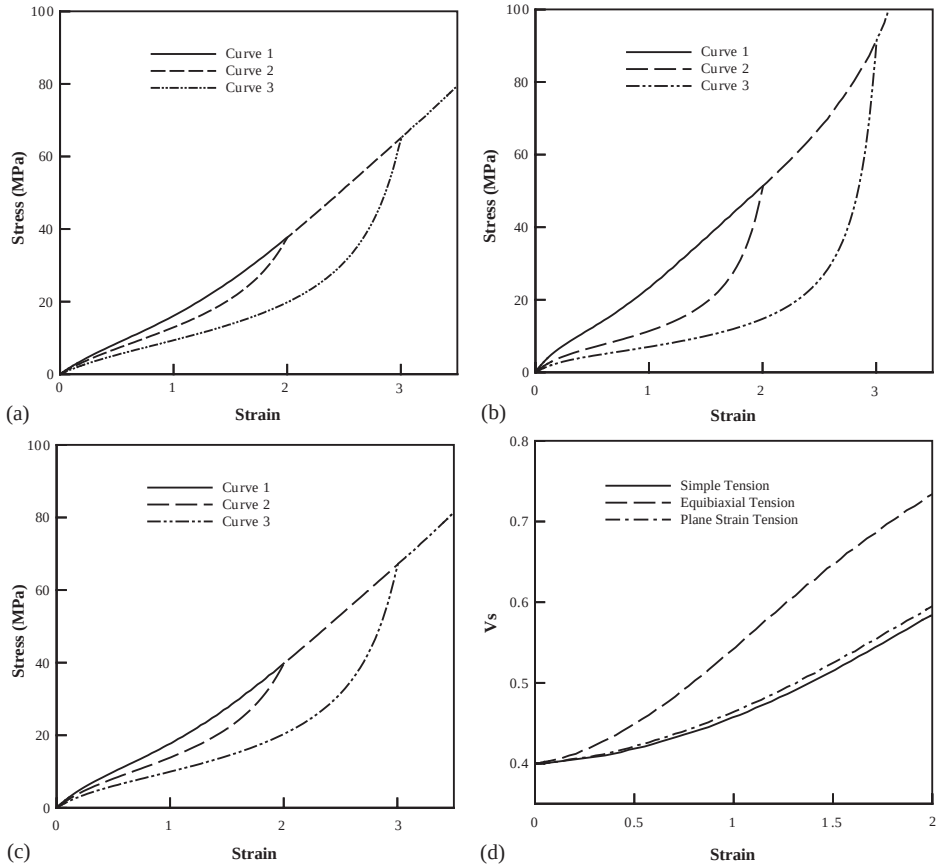

Fig. 4. The nominal stress-nominal strain curves for (a) the uniaxial tension test; (b) the equibiaxial tension test; (c) the plane strain tension test; (d) the evolution in effective volume fraction of soft domains in the three tests during the first virgin material loading to $\varepsilon = 2.0$.

where $\Lambda_{\text{chain}} = \sqrt{\frac{X}{3}(2\lambda^2 + \lambda^{-4} - 3) + 1}$, and $\lambda_1 = \lambda_2 = \lambda$ is the equibiaxial tension. Fig. 4(b) shows the cyclic nominal stress-nominal strain curves for equibiaxial tension. In equibiaxial tension, at any given strain, the material is subjected to a higher molecular chain stretch than at that same strain in uniaxial tension. Therefore, the material shows a greater amount of softening (a more compliant response) during reloading under equibiaxial tensile conditions when compared to uniaxial tensile conditions. The evolution in the volume fraction of soft domains with the different loading states is shown in Fig. 4(d). Clearly, equibiaxial tensile conditions show a larger volume fraction of soft domain at any given strain.

The nominal stress–stretch behavior in plane strain tension is given by

$$f_1 = \frac{v_s X \mu}{3} \frac{\sqrt{N}}{\Lambda_{\text{chain}}} \mathsf{L}^{-1}\left(\frac{\Lambda_{\text{chain}}}{\sqrt{N}}\right)(\lambda - \lambda^{-3}), \tag{19}$$

where $\Lambda_{\text{chain}} = \sqrt{\frac{X}{3}(\lambda^2 + \lambda^{-2} - 2) + 1}$, and $\lambda_1 = \lambda$ is the axial stretch. Fig. 4(c) shows the cyclic nominal stress-nominal strain curves for plane strain tension. In plane strain tension, at a given axial strain, the material is subjected to a slightly higher molecular chain stretch than when in uniaxial tension. Therefore, the material shows a slightly more compliant response during reloading. Fig. 4(d) shows the evolution of effective volume fraction of soft domains during each of the tests.

4. Conclusion

A constitutive model accounting for the stretch-induced softening behavior is presented in this paper. For the softening of the equilibrium path, the model adopts the Mullins and Tobin concept of an evolution in the underlying hard and soft domain microstructure whereby the volume fraction of soft domain undergoing deformation increases with stretch due to structural reorganization of the soft and hard domains. The concept of amplified strain is then utilized in a mapping of the macroscopic deformation to the deformation experienced by the soft domain. The strain energy density function of the material is then taken to be derived from the strain energy of the soft domain and thus evolves as the volume fraction of soft domain evolves with deformation. Comparisons of model results for cyclic uniaxial extension are found to favorably compare with the experimental data of Mullins and Tobin. Model predictions for the equilibrium stress–strain behavior and corresponding evolution in soft domain during cyclic stretching under different states of stretch are also presented, demonstrating the fully three-dimensional capabilities of the model. The efficacy of this softening model as a softening element within nonlinear viscoelastic models of large strain time dependent behavior of elastomeric-like material is discussed in Qi and Boyce (2004).

Appendix A. Formulation of Cauchy stress tensor

From the 2nd law of thermodynamics, the Clausius Duhem inequality for an isothermal process can be written as

$$\tfrac{1}{2}\,\tilde{\mathbf{T}} \bullet \dot{\mathbf{C}} - \dot{U} \geqslant 0 \tag{A.1}$$

as expressed in term of work conjugate 2nd Piola Kirchhoff stress $\tilde{\mathbf{T}} = \det(\mathbf{F})\mathbf{F}^{-1}\mathbf{T}\mathbf{F}^{\mathrm{T}-1}$ and the right Cauchy Green tensor $\mathbf{C} = \mathbf{F}^{\mathrm{T}}\mathbf{F}$. U is the free energy, and in the proposed model, is defined to be a function of overall chain stretch I_1 and the internal variable v_s

$$U = U(I_1, v_s). \tag{A.2}$$

From Eq. (A.2),

$$\dot{U} = \frac{\partial U}{\partial I_1}\frac{\partial I_1}{\partial \mathbf{C}} \bullet \dot{\mathbf{C}} + \frac{\partial U}{\partial v_s}\dot{v}_s. \tag{A.3}$$

Then the inequality (A.1) gives

$$\left(\frac{1}{2}\tilde{\mathbf{T}} - \frac{\partial U}{\partial I_1}\frac{\partial I_1}{\partial \mathbf{C}}\right) \bullet \dot{\mathbf{C}} - \frac{\partial U}{\partial v_s}\dot{v}_s \geqslant 0. \tag{A.4}$$

For an arbitrary deformation,

$$\tilde{\mathbf{T}} = 2\frac{\partial U}{\partial I_1}\frac{\partial I_1}{\partial \mathbf{C}} \tag{A.5a}$$

and

$$-\frac{\partial U}{\partial v_s}\dot{v}_s \geqslant 0. \tag{A.5b}$$

By taking into account the incompressibility of the material, Eq. (A.5a) gives the 2nd Piola Kirchhoff stress,

$$\tilde{\mathbf{T}} = 2\frac{\partial U}{\partial I_1}\frac{\partial I_1}{\partial \mathbf{C}} - p\mathbf{C}^{-1}. \tag{A.6}$$

Then the Cauchy stress is

$$\mathbf{T} = -p\mathbf{I} + 2\frac{\partial U}{\partial I_1}\mathbf{B}. \tag{A.7}$$

For the strain energy function used in the main text,

$$U = v_s\mu\left[\sqrt{N}\Lambda_{\text{chain}}\beta + N\ln\frac{\beta}{\sinh\beta}\right]. \tag{A.8}$$

Eq. (A.7) gives the Cauchy stress as

$$\mathbf{T} = \frac{v_s X\mu}{3}\frac{\sqrt{N}}{\Lambda_{\text{chain}}}\mathsf{L}^{-1}\left(\frac{\Lambda_{\text{chain}}}{\sqrt{N}}\right)\mathbf{B} - p\mathbf{I}. \tag{A.9}$$

Inequality (A.5b) shows the evolution of effective volume fraction is an energy dissipation process. For the proposed constitutive model, when $\dot{v}_s > 0$, $\partial U/\partial v_s < 0$, and Eq. (A.5b) is satisfied; when $\dot{v}_s = 0$, $\partial U/\partial v_s = 0$, and Eq. (A.5b) is also satisfied.

Inequality (A.5b) shows the conversion of hard domains to soft domains is an irreversible and dissipative process, which is consistent with the assumptions used in both damage based and phase transition based models where the damage or phase transition is an irreversible process (Govindjee and Simo, 1991, 1992; Miehe and Keck, 2000; Beatty and Krishnaswamy, 2000; Marckmann et al., 2002; Ogden and Roxburgh, 1999a,b; Dorfmann and Ogden, 2003). The fact that domain transition is irreversible was also observed in the study of segmented thermoplastic polyurethane elastomers (Yokoyama, 1978; Bonart and Muller-Riederer, 1981), which also demonstrates strong stretch induced softening behavior (Qi and Boyce, 2004).

Table 3
The $v_s^{(i)}$s and corresponding $\Lambda_{chain}^{(i)}$ for Mullins and Tobin results

i	$v_s^{(i)}$	$\Lambda_{chain}^{(i)}$
1	0.5	2.42
2	0.6	3.57
3	0.72	4.03
4	0.8	4.27

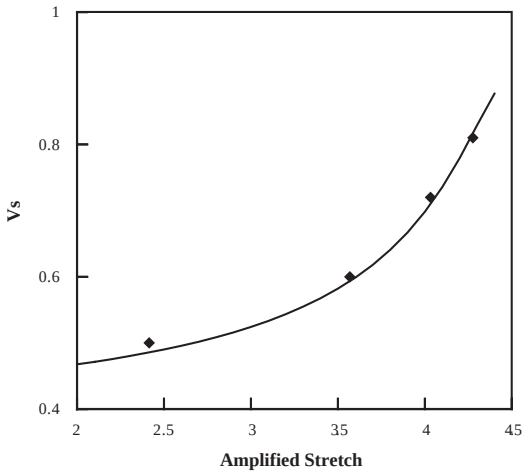

Fig. 5. $v_s^{(i)} - \Lambda_{chain}^{(i)}$ plot. The diamond symbols are from the $v_s^{(i)}$ obtained by best fitting reloading curves. The solid line is from the best fitting of the $v_s^{(i)} - \Lambda_{chain}^{(i)}$ plot using Eq. (16).

Appendix B. Material parameter identification

The material properties include the material properties of the soft domain, μ and N, and the softening properties of the initial volume fraction of soft domain v_{s0}, the final/saturated volume fraction of soft domain v_{ss}, and the evolution coefficient A. In order to obtain the properties of the soft domain, it is best to use the reloading curve that has the largest maximum previously attained strain. In the Mullins and Tobin results, reloading occurs after $\varepsilon_1 = 1.0$, $\varepsilon_2 = 2.0$, $\varepsilon_3 = 3.0$, and $\varepsilon_4 = 4.0$. Here, we use the curve corresponding to $\varepsilon_4 = 4.0$ to exemplify this procedure.

The data suggest that additional softening would occur if the material were strained beyond a strain of 4.0, therefore, we estimate the volume fraction of soft domain after a strain of 4.0 to be $v_s^{(4)} \approx 0.80$, giving a corresponding amplification factor of $X^{(4)} = 2.42$. The parameters μ and N are determined to be $\mu = 1.94$ MPa and $N = 21.0$ by best fitting the reloading curve using the proposed model with $v_s^{(4)} = 0.80$. The locking chain stretch hence is $\lambda_{chain}^{locking} = \sqrt{N} = 4.58$.

The ratio between the initial Young's moduli of the virgin material curve and the reloading curve is measured to be $E_0^{(0)}/E_0^{(1)} = 1.95$. From Eq. (14), for uniaxial tension,

$$E_0 = v_s X \mu. \tag{B.1}$$

Therefore,

$$\frac{E_0^{(0)}}{E_0^{(4)}} = \frac{v_{s0} X^{(0)}}{v_s^{(4)} X^{(4)}} = \frac{v_{s0}[1 + 3.5(1 - v_{s0}) + 18(1 - v_{s0})^2]}{v_s^{(4)}[1 + 3.5(1 - v_s^{(4)}) + 18(1 - v_s^{(4)})^2]}, \tag{B.2}$$

a value for v_{s0} is obtained and found to be 0.44.

The parameters v_{ss} and A can thus be obtained to be $v_{ss} = 0.9$ and $A = 0.15$ by fitting the loading curve of virgin material with $\mu = 1.94$ MPa, $N = 21.0$, and $v_{s0} = 0.44$.

As an alternative property fitting protocol, the parameters v_{ss} and A can be determined from the reloading curves at different maximum strains seen in its prior strain history. In the Mullins and Tobin results, reloading occurs after $\varepsilon_1 = 1.0$, $\varepsilon_2 = 2.0$, $\varepsilon_3 = 3.0$, and $\varepsilon_4 = 4.0$. Using $\mu = 1.94$ MPa and $N = 21.0$ and $v_s^{(4)} = 0.80$, the $v_s^{(i)}$ $(i = 1, 2, 3)$ can be obtained by best fitting each reloading curve using the proposed model. Table 3 lists the $v_s^{(i)}$ and corresponding $\Lambda_{\text{chain}}^{(i)}$. By best fitting the $v_s^{(i)} - \Lambda_{\text{chain}}^{(i)}$ plot, we obtained $v_{ss} = 0.9$ and $A = 0.16$, which is very close to the value obtained by fitting the loading curve. Fig. 5 shows the $v_s^{(i)} - \Lambda_{\text{chain}}^{(i)}$ plot, where curve 1 is from the $v_s^{(i)}$ obtained by fitting the reloading curves and curve 2 is from the best fitting of the $v_s^{(i)} - \Lambda_{\text{chain}}^{(i)}$ plot using Eq. (16).

References

Arruda, E.M., Boyce, M.C., 1993. A three-dimensional constitutive model for the large stretch behavior of elastomers. J. Mech. Phys. Solids 41, 389–412.

Beatty, M.F., Krishnaswamy, S., 2000. A theory of stress-softening in incompressible isotropic materials. J. Mech. Phys. Solids 48, 1931–1965.

Bergstrom, J., Boyce, M.C., 1999. Mechanical behavior of particle filled elastomers. Rubber Chem. Tech. 72, 633–656.

Bergstrom, J.S., Boyce, M.C., 2000. Large strain time-dependent behavior of filled elastomers. Mech. Mater. 32, 627–644.

Blanchard, A.F., Parkinson, D., 1952. Breakage of carbon-rubber networks by applied stress. Ind. Eng. Chem. 44, 799.

Bonart, R., Muller-Riederer, G., 1981. Modelvorstellungen zue Molekulorientierung in gedehnten segmentierten polyurehan-elastomeren. Colloid Polym. Sci. 259, 926–936.

Boyce, M.C., Socrate, S., Yeh, O.C., Kear, K., Shaw, K., 2001a. Micromechanisms of deformation and recovery in thermoplastic vulcanizates. J. Mech. Phys. Solids 49, 1073–1098.

Boyce, M.C., Yeh, O.C., Socrate, S., Kear, K., Shaw, K., 2001b. Micromechanisms of the cyclic softening in thermoplastic vulcanizates. J. Mech. Phys. Solids 49, 1343–1360.

Budiansky, B., 1965. On the elastic moduli of some heterogeneous materials. J. Mech. Phys. Solids 13, 223–227.

Bueche, F., 1960. Molecular basis for the Mullins effect. J. Appl. Polym. Sci. 4, 107–114.

Bueche, F., 1961. Mullins effect and rubber-filler interaction. J. Appl. Polym. Sci. 5, 271–281.

Dannenberg, E.M., 1974. The effects of surface chemical interactions on the properties of filler-reinforced rubbers. Rubber Chem. Technol. 48, 410–444.

Dorfmann, A., Ogden, R.W., 2003. A pseudo-elastic model for loading, partial unloading and reloading of particle-reinforced rubber. Int. J. Solids Struct. 40, 2699–2714.

Einstein, A., 1906. Eine neue bestimmung der molekuldimensionen. Ann. Phys. (Leipzig) 19, 289.

Einstein, A., 1911. Berichtigung zu meiner arbeit: Eine neue bestimmung der molekuldimensionen. Ann. Phys. (Leipzig) 34, 591.

Govindjee, S., Simo, J., 1991. A micro-mechanically based continuum damage model for carbon black-filled rubbers incorporating Mullins' effect. J. Mech. Phys. Solids 39, 87–112.

Govindjee, S., Simo, J., 1992. Transition from micro-mechanics to computationally efficient phenomenology: carbon black filled rubbers incorporating Mullins' effect. J. Mech. Phys. Solids 40, 213–233.

Guth, E., 1945. Theory of filler reinforcement. J. Appl. Phys. 16, 20.

Guth, E., Gold, O., 1938. On the hydrodynamical theory of the viscosity of suspensions. Phys. Rev. 53, 322.

Guth, E., Simha, R., 1936. Untersuchungen uber die viskositat von suspension und losungen 2. uber die viskositat von kugelsuspensionen. Kolloid-Z 74, 266.

Harwood, J.A.C., Payne, A.R., 1966a. Stress softening in natural rubber vulcanizates, Part III. J. Appl. Polym. Sci. 10, 315–324.

Harwood, J.A.C., Payne, A.R., 1966b. Stress softening in natural rubber vulcanizates, Part IV. J. Appl. Polym. Sci. 10, 1203–1211.

Harwood, J.A.C., Mullins, L., Payne, A.R., 1965. Stress softening in natural rubber vulcanizates, Part II. J. Appl. Polym. Sci. 9, 3011–3021.

Horgan, C.O., Ogden, R.W., Saccomandi, G., 2004. A theory of stress softening of elastomers based on finite chain extensility. Proc. R. Soc. London, Ser. A, to appear.

James, A.G., Green, A., 1975. Strain energy functions of rubber. II. Characterization of filled vulcanizates. J. Appl. Polym. Sci. 19, 2319–2330.

Johnson, M.A., Beatty, M.F., 1993a. The Mullins' effect in uniaxial extension and its influence on the transverse vibration of a rubber string. Continuum Mech. Thermodyn. 5, 83–115.

Johnson, M.A., Beatty, M.F., 1993b. A constitutive equation for the Mullins effect in stress controlled uniaxial extension experiments. Continuum Mech. Thermodyn. 5, 301–318.

Lion, A., 1996. A constitutive model for carbon black filled rubber, experimental investigation and mathematical representation. Continuum Mech. Thermodyn. 6, 153–169.

Lion, A., 1997. A physically based method to represent the thermo-mechanical behavior of elastomers. Acta Mech. 123, 1–25.

Marckmann, G., Verron, E., Gornet, L., Chagnon, G., Charrier, P., Fort, P., 2002. A theory of network alteration for the Mullins effect. J. Mech. Phys. Solids 50, 2011–2028.

Medalia, A.I., Kraus, G., 1994. Science and Technology of Rubber. Academic Press Inc., New York, p. 387.

Miehe, C., Keck, J., 2000. Superimposed finite elastic-viscoelastic-plastoelastic response with damage in filled rubbery polymers. Experiments, modeling and algorithmic implementation. J. Mech. Phys. Solids 48, 323–365.

Mori, T., Tanaka, K., 1973. Average stress in matrix and average elastic energy of materials with misfitting inclusions. Acta Metall. 21, 571–574.

Mullins, L., 1948. Effect of stretching on the properties of rubber. Rubber Chem. Technol. 21, 281–300.

Mullins, L., 1969. Softening of rubber by deformation. Rubber Chem. Technol. 42, 339–362.

Mullins, L., Tobin, N.R., 1957. Theoretical model for the elastic behavior of filler-reinforced vulcanized rubber. Rubber Chem. Technol. 30, 555–571.

Mullins, L., Tobin, N.R., 1965. Stress softenings in natural rubber vulcanizates, Part I. J. Appl. Polym. Sci. 9, 2993–3010.

Ogden, R.W., Roxburgh, D.G., 1999a. A pseudo-elastic model for the Mullins effect in filled rubber. Proc. R. Soc. London, Ser. A 455, 2861–2877.

Ogden, R.W., Roxburgh, D.G., 1999b. An energy-based model of the Mullins effect. Proceedings of the First European Conference on Constitutive Models for Rubber, Belkema, Rotterdam.

Ponte Castaneda, P., 1989. The overall constitutive behavior of nonlinearly elastic composites. Proc. R. Soc. London, Ser. A 422, 147–171.

Qi, H.J., Boyce, M.C., 2004. Stress strain behavior of thermoplastic polyurethane. Mech. Mater., submitted for publication.

Rajagopal, K.R., Wineman, A.S., 1992. A constitutive model for nonlinear solids which undergo deformation induced microstructural changes. J. Plasticity 8, 385–395.

Rigbi, Z., 1980. Reinforcement of rubber by carbon black. Adv. Polym. Sci. 36, 21–68.

Simo, J.C., 1987. On a fully three-dimensional finite-strain viscoelastic damage model: formulation and computational aspects. Comput. Method Appl. Mech. Eng. 60, 153–173.

Smallwood, H.M., 1944. Limiting law of the reinforcement of rubber. J. Appl. Phys. 15, 758.

Suquet, P., 1997. Effective properties of nonlinear composites. In: Suquet, P. (Ed.), Continuum Micromechanics. Springer-Wien, New York.

Wineman, A.S., Huntley, H.E., 1994. Numerical simulation of effect of damaged induced softening on the inflation of a circular rubber membrane. Int. J. Solids Struct. 31, 3295–3313.

Yokoyama, T., 1978. Elasticity and structure of polyurethane networks. In: Frisch, K.C., Reegen, S.L. (Eds.), Advances in Urethane Science and Technology. Technomic Publishing Co., Westport, CT.